




## Influence of molecular weight on the distribution of segmental relaxation in polymer grafted nanoparticles

Aakash Sharma <sup>1,\*</sup>, Margarita Kruteva <sup>1,†</sup>, Michaela Zamponi,<sup>2</sup> Sascha Ehlert <sup>1</sup>, Dieter Richter,<sup>1</sup> and Stephan Förster<sup>1</sup>

<sup>1</sup>Forschungszentrum Jülich GmbH, Jülich Centre for Neutron Science (JCNS-I: Neutron Scattering and Biological Matter), 52425 Jülich, Germany

<sup>2</sup>Forschungszentrum Jülich GmbH, Jülich Centre for Neutron Science at MLZ, Lichtenbergstraße 1, 85748 Garching, Germany



(Received 4 July 2021; revised 5 October 2021; accepted 12 January 2022; published 25 January 2022)

The segmental dynamics of one-component nanocomposites (OCNC) is significantly influenced by the molecular weight ( $M_w$ ) of the grafted polymer. Neutron backscattering shows that compared to the neat polymer the OCNCs exhibit a shift from slower segmental dynamics at low  $M_w$  to faster dynamics at high  $M_w$ . We model the local relaxation as distribution of exponential diffusers. This approach reveals the presence of fast and slow segments in both OCNCs. However, their fractional contribution varies with  $M_w$  leading to different average relaxation times. Our results present important insights into the origin of segmental mobility in OCNC and address the inconsistencies in different literature reports.

DOI: [10.1103/PhysRevMaterials.6.L012601](https://doi.org/10.1103/PhysRevMaterials.6.L012601)

One-component nanocomposites (OCNC) made from polymer grafted nanoparticles are an advanced class of nanocomposite materials, which circumvent the problem of segregation, commonly encountered in conventional nanocomposites. OCNC are known for widely tunable properties like strength, flexibility, etc., making them suitable for processing industry [1,2] and candidates for applications in energy storage, drug carriers, gas separation, etc. [3–5]. Properties and processability of nanocomposites are dependent on the dynamics of polymer chains at different length scales. For example, processability is governed by their melt-state viscosity, which is controlled by the entanglements dynamics [6]. Similarly, the diffusion of gas molecules through membranes made from one-component nanocomposites depends on the dynamics of the grafted polymer segments at short length scales [7]. Therefore, a thorough investigation of polymer dynamics is essential not only from the perspective of fundamental study but also from an application point of view.

Dynamics can be probed using techniques like rheology, dielectric spectroscopy, etc. Under this category, quasielastic neutron spectroscopy (QENS) stands out as a powerful tool to quantify dynamics at different length scales of a polymer chain [8]. Quasielastic neutron backscattering is well utilized to explore the segmental dynamics at length scales on the order of a nanometer in polymers [9], which is a decisive factor for properties like glass transition temperature ( $T_g$ ), gas permeability, conductivity, etc. [7,9–11]. Polymer melts like polyisoprene, polybutadiene, poly(methylmethacrylate), and others show a Gaussian distribution of segmental displacements at low scattering vectors ( $Q$ ) and local diffusion at higher  $Q$  [12–16]. On the other hand, in a grafted state polymer chains experience spatially variable conformations

as a function of distance from the particle surface [17–20]. Grafting induces restricted mobility at the anchor site, which alters the local conformation of polymer chains and indirectly governs the center to center distance of nanoparticles [17]. Recently, a two-layer model presented by Midya *et al.* [17] assumes that for higher grafting density the polymer layers close to the particle surface are stretched, resulting in a dry, not accessible layer around the nanoparticle, whereas segments away from the surface interpenetrate. Alteration of segmental conformation by grafting eventually affects their dynamics.

A decrease of the chain relaxation rate on grafting is commonly observed [21–25]. However, there are two contradictory views on the segmental dynamics. There are reports showing an overall similar or decreasing segmental relaxation rate for grafted polymers [20,22]. However, other results show nonintuitive acceleration of the segmental relaxation [7,26,27]. Using backscattering experiments on polyisoprene grafted silica particles our group showed that grafting does not alter the segmental dynamics in OCNCs [20]. However, Jhalaria *et al.* reported faster segmental dynamics for poly(methylacrylate) grafted silica particles as compared to pure polymer [7]. We note that both reports study the average segmental relaxation. However, one anticipates that the segments closer to the particle surface are retarded as compared to those near the chain ends. Other than in chemistry, these two reports differ in the molecular weights and grafting densities of the polymer. We explore these factors in experiments on densely grafted polymer chains (about  $3\times$  above those of Ref. [7]) for two different molecular weights. Our results demonstrate a dramatic shift of the backscattering relaxation times with molecular weights of the grafted chains. We also study the effect of temperature on segmental dynamics, which is an important factor for an application of interest. In order to obtain correct quantities, a careful inclusion of all dynamic processes, in particular methyl side group motion, is mandatory, which we demonstrate in the current work.

\*a.sharma@fz-juelich.de

†m.kruteva@fz-juelich.de

Major outcomes of this study are as follows: Compared to the neat polymer at equal grafting density (i) low molecular weight OCNC display delayed local relaxation, while (ii) at high molecular weight faster segmental dynamics is observed in backscattering. An analysis of the relaxation time spectra reveals the presence of fast segments for both OCNC. However, the fractional contribution of decelerated segments varies with molecular weight, leading to qualitatively different average relaxation times in nanocomposites of different molecular weights. With this observation we resolve apparently contradictory results in the literature. Our analysis results are also applicable for other similar systems, e.g., in the study of reinforced rubber [28].

Polyisoprene (PI) of two different molecular weights, 5000 g/mole (PI-5k) and 12000 g/mole (PI-12k), was grafted on narrow disperse iron oxide nanoparticles with diameter =  $9.4 \pm 1$  nm, synthesized via conventional thermal degradation of iron oleate. Polymer grafted nanoparticles were obtained via the ligand exchange method [29]. Respective one-component nanocomposites (NC-5k and NC-12k) were used for QENS experiments. Details of the polymerization, nanoparticles synthesis, grafting procedure, and characterizations were published separately [29]. The grafting densities for both NC-5k and NC-12k amount to 1.5 chains/nm<sup>2</sup> [see Supplemental Material (SM [30])]. Neutron backscattering experiments were performed on all samples at 275 and 300 K on SPECTROMETER for High Energy RESolution (SPHERES) (energy resolution =  $0.65 \mu\text{eV}$ ) at Maier-Leibnitz Zentrum (MLZ) [31]. We used the energy range  $-30 < \hbar\omega < 30 \mu\text{eV}$  with  $\lambda = 6.271 \text{ \AA}$ . Backscattering spectra were normalized for detector efficiencies using a vanadium reference. Empty cell scattering was subtracted as background. Spectra obtained at 3 K for each sample were used to determine the instrument resolution, which was convoluted with the model function during fitting. Corrected data were fitted in the frequency domain USING JSCATTER software [32] that bases on Fourier-transformed double Kohlrausch-Williams-Watts (KWW) function:

$$S_{\text{KWW}}(Q, \omega) = \mathcal{F} \left\{ \chi \left[ \text{Amp} \times \exp \left[ - \left( \frac{t}{\tau(Q)} \right)^\beta \right] \right] + (1 - \chi) \left[ \text{Amp} \times \exp \left[ - \left( \frac{t}{\tau_2} \right)^\beta \right] \right] \right\}, \quad (1)$$

where  $S_{\text{KWW}}(Q, \omega)$  is the scattering function,  $\chi$  is fractional contribution of mobile polymer layer,  $t$  is time,  $\tau$  is  $Q$ -dependent KWW relaxation time,  $\tau_2$  is fixed at a high value ( $>6500$  ns), thereby effectively describing the resolution function. The elastic part of the spectra relates to protons of surface ligands, and the nanoparticles themselves,  $\beta$  is the stretching parameter, and Amp is an amplitude factor. For neat polymer samples,  $\chi = 1$ . Measurements were made at different  $Q$  values varying from 0.60 to  $1.66 \text{ \AA}^{-1}$ . Adequate resolution functions are indicated as dotted lines in the figures.

Figure 1 shows representative backscattering spectra of PI-5k and NC-5k at 300 K and  $Q = 1.12 \text{ \AA}^{-1}$ . We observe that the OCNC show additional elastic scattering in the low-energy region. Consequently, a single KWW function fails to capture the entire spectrum. Our group has shown previously that in polyisoprene grafted SiO<sub>2</sub> nanoparticles the dynamics of about 3 monomers close to the grafting site is slowed down

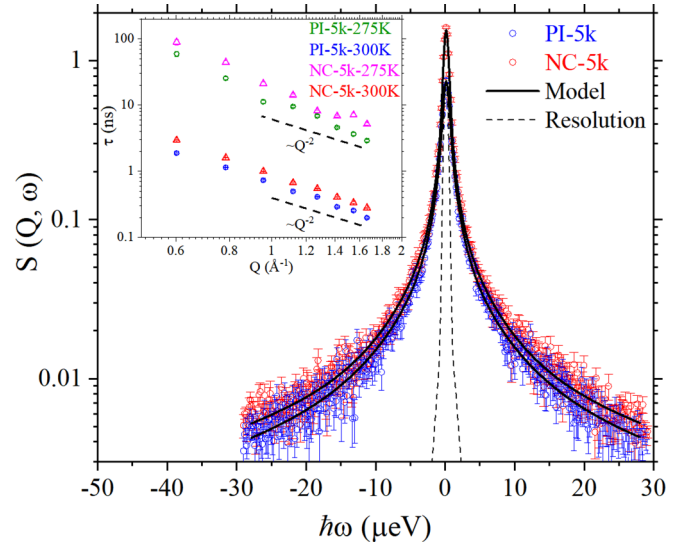


FIG. 1. Fitted backscattering spectra for polyisoprene, 5000 g/mole and its nanocomposite obtained at 300 K and  $Q = 1.12 \text{ \AA}^{-1}$ . Inset shows relaxation times from PI-5k and NC-5k at 275 and 300 K for different  $Q$ .

significantly and therefore contributes to the elastic component in backscattering [20]. We note here that these segments do not contribute to quasielastic scattering in the frequency range of the spectrometer and should not be interpreted as completely frozen [33]. Dynamics of segments away from the particle surface is quantifiable in the backscattering window. To fit the nanocomposite spectra presented in Fig. 2(a) we use double KWW function of Eq. (1) and allow  $\chi$  to vary with  $Q$ . The mobile fraction obtained for 300 K is 0.91 and was fixed for low-temperature fit, assuming thereby that the elastic fraction in the spectrum does not change with temperature. An elastic fraction of 0.09 translates into a layer thickness of

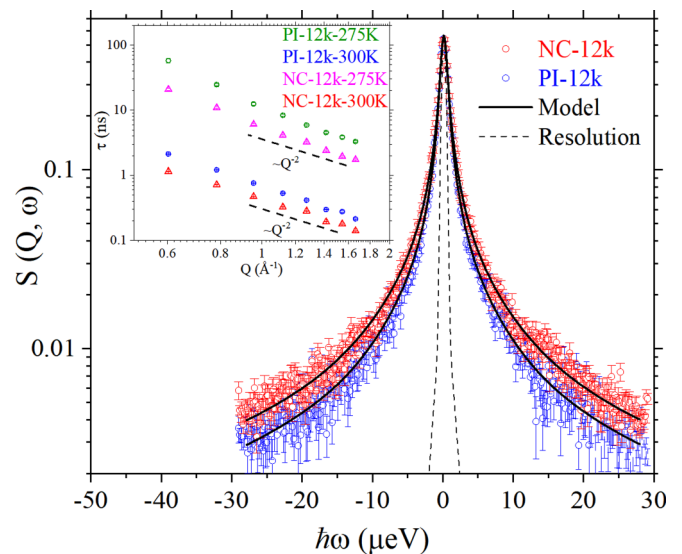


FIG. 2. Fitted backscattering spectra for polyisoprene, 12 000 g/mole and its nanocomposite obtained at 300 K and  $Q = 1.12 \text{ \AA}^{-1}$ . Inset shows relaxation times from PI-12k and NC-12k at 275 and 300 K for different  $Q$ .

about 1 nm of slow segments, which is in line with previous studies [7,20].

Equation (1) assumes that the relaxation process captured in the backscattering data originates primarily from the backbone segments. Other faster processes, e.g., methyl group rotation, thermal vibrations, etc., contribute only to an initial decay in the relaxation, thus merely changing the amplitude (Amp). This assumption is adequate for measurements at 300 K. However, at 275 K, the methyl rotation retards sufficiently and is captured in the backscattering energy range, which renders this assumption invalid. We account for the scattering from methyl rotation as described in the literature [34]:

$$S_{\text{methyl}}(Q, \omega) = \mathcal{F}\{(1 - A(Q))\Phi(t) + A(Q)\}, \quad (2)$$

where  $A(Q)$  is the elastic incoherent structure factor from the processes that are *apparently frozen* in the backscattering window and  $\Phi(t)$  is the reorientation relaxation of methyl (details in SM [30]).  $S_{\text{methyl}}(Q, \omega)$  in Eq. (2) was calculated at 275 K based on the values provided in Refs. [34,35]. The resulting scattering process is described as a convolution of KWW function and methyl relaxation process [16], i.e.,  $S(Q, \omega) = S_{\text{KWW}}(Q, \omega) \otimes S_{\text{methyl}}(Q, \omega)$ . The corresponding relaxation times of the mobile fraction are shown in the inset of Fig. 1. At both 275 and 300 K, the segment relaxation times in the OCNC are longer than those of the neat polymer, indicating retardation of segmental dynamics.

We compare our results with literature reports on similar materials. In the past we showed that grafting of polyisoprene (M.W.  $\sim 5000$  g/mole) on silica particles does not affect the segmental relaxation within the mobile polymer layer [20]. However, those results were obtained at a substantially lower grafting density of 0.59 chains/nm<sup>2</sup> as compared to our current grafting density of 1.5 chains/nm<sup>2</sup>. Results presented here and in previous report [20] suggest that the segmental relaxation rates of grafted chains are also a function of grafting density. We note that our results appear to contradict the literature report [7], where the authors have found an increase in the segmental motion of poly(methylacrylate) chains grafted on silica nanoparticles for different molecular weight of grafted polymer. However, the molecular weights of the polymers reported there were much higher than that reported in Fig. 1.

We now explore the segmental relaxation of higher molecular weight polyisoprene (12 000 g/mole) grafted iron oxide particles. Figure 2 shows the comparison of backscattering spectra obtained from PI-12k and NC-12k for  $Q = 1.12 \text{ \AA}^{-1}$  at 300 K. In contrast to the NC-5k samples, we could fit the data from NC-12k samples using a single KWW function ( $\chi = 1$ ) for all  $Q$  values. However, NC-12k samples are also bound to exhibit a layer of low mobility. To take it into account, we fix the number of segments giving rise to an elastic component on the basis of the NC-5k sample for NC-12k to  $\chi = 0.96$ . Figure 2, inset shows that NC-12k exhibits shorter relaxation times than PI-12k at 275 and 300 K. Our results for the higher molecular weight nanocomposite are in qualitative agreement with those reported by Jhalaria *et al.* [7] who obtained faster KWW relaxation times for the grafted polymer. We note that, although the data could be fitted using a single KWW function ( $\chi = 1$ ), to obtain accurate values for relaxation time, one

must consider the presence of a slow layer in higher molecular weight samples too.

We notice a qualitative difference between the low molecular weight (NC-5k) and high molecular weight nanocomposites. In NC-5k, the nanocomposites exhibit a slower segmental relaxation than the corresponding polyisoprene samples, whereas, NC-12k samples exhibit faster relaxation than PI-12k. The segmental relaxation in neat polyisoprene remains unaffected by the molecular weight as shown in the SM (Fig. S1) [30]. These comparisons are also confirmed by the average relaxation times ( $\tau_0 = \frac{\tau}{\beta} \Gamma[\frac{1}{\beta}]$ ) (Fig. S2, SM [30]). We reemphasize that other by an elastic contribution the QENS spectra do not account for the segments present in the surface polymer layer. The stretching parameter for neat polyisoprene and OCNC at 300 K is  $0.45 < \beta < 0.52$  and at 275 K is  $0.35 < \beta < 0.45$ , which are in agreement with the values reported in literature [13]. We do not notice significant changes in  $\beta$  from neat polymer to nanocomposites. All samples show slower dynamics at 275 K as compared to 300 K, which is as anticipated. We obtained glass transition temperature  $T_g$  using differential scanning calorimetry measurements (Fig. S4, SM [30]) and notice an increase in  $T_g$  on grafting from PI-5k (208.5 K) to NC-5k (210.39 K), whereas, from PI-12k (210.2 K) to NC-12k (208.33 K)  $T_g$  decreases. This is in line with the relaxation time results.

The alteration of OCNC segmental relaxation from faster to slower dynamics in comparison to the neat polymer with decreasing molecular weight of grafted polymer is counterintuitive. The spatial underpinnings of this finding must lie in the heterogeneity of local mobility along the grafted polymer chain. However, conventional method of analyzing QENS data by fitting a KWW function fails to provide sufficient information in this respect and therefore, an improved analysis method is essential. In order to develop a better understanding of the relaxation mechanism, we inspect the variation of relaxation times with  $Q$  shown in the insets of Figs. 1 and 2 and in Fig. S3 (SM [30]). We notice that the relaxation times exhibit a  $Q^{-2}$  dependence at high  $Q$  and  $Q^{-4}$  dependence at low- $Q$  values (Figs. S1 and S3, SM [30]), which agrees with the results published by Arbe *et al.* [13,14]. For polyisoprene in the literature, the crossover from Gaussian to non-Gaussian dynamics has been shown to occur around  $Q = 1 \text{ \AA}^{-1}$  [13,14]. We propose that the deviation from a clear crossover at  $1 \text{ \AA}^{-1}$  in our case most likely relates to multiple scattering effect [15]. Nevertheless, a variation of relaxation times as  $Q^{-2}$  suggests that the underlying relaxation process can be described as an exponential process like simple diffusion [15,36]. Hence, the segmental dynamics of the mobile polymer fraction can be modeled as a superposition of segments exhibiting short time diffusion with distributed relaxation times. Although the KWW parameters, i.e.,  $\tau$  and  $\beta$ , provide an overview of the distributed timescales, details like change in shape, symmetry, etc., however, are lumped into these parameters. In order to gain deeper understanding, we follow the work of Alvarez *et al.* [37] and use the CONTIN regularization approach to obtain the relaxation time spectra for the mobile layer [38,39]. We choose data between  $1.27 \text{ \AA}^{-1} < Q < 1.66 \text{ \AA}^{-1}$  to evaluate the relaxation time spectra. We note that the distribution of single diffusers is not valid for low- $Q$  data as the relaxation time does not vary as  $Q^{-2}$ ; hence, the governing re-



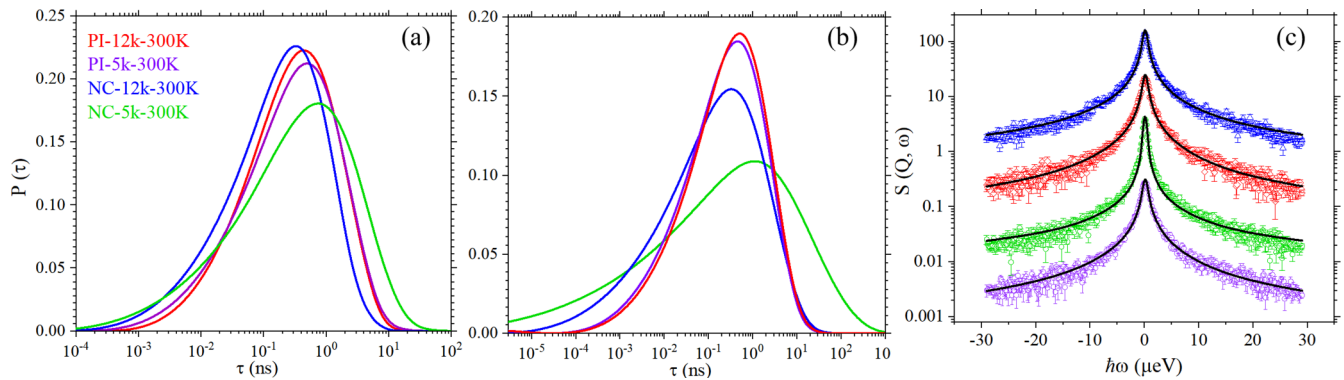


FIG. 3. Comparison of relaxation time spectra for PI-5k, NC-5k, PI-12k, and NC-12k at 300 K from (a) backscattering at  $Q = 1.4 \text{ \AA}^{-1}$ , (b) dielectric spectroscopy, and (c) vertically shifted backscattering data at 300 K and  $Q = 1.4 \text{ \AA}^{-1}$ . The black lines indicate the data description on the basis of the shifted dielectric relaxation time spectra.

relaxation process cannot be modeled by a distribution of single exponentials.

Figure 3(a) compares the relaxation time spectra of the pure melt and the OCNC at 300 K for  $Q = 1.4 \text{ \AA}^{-1}$ . The distribution of relaxation times for NC-5k is extended to longer timescales. Interestingly, also indications of an increased contribution of faster (short time) segments could be observed for all  $Q$  values (Fig. 3(a) and Fig. S8, SM [30]). At 275 K (Fig. S7, SM [30]) short time response is similar in PI-5k and NC-5k. For NC-12k the entire spectrum moves to shorter timescales. The comparison of the OCNC relaxation time spectra evidences that the difference in the dynamics of NC-5k and NC-12k is strongly influenced by slow relaxing components. NC-5k exhibits substantially higher fraction of slower segments than NC-12k. While the general features of the distributions do not depend on  $Q$ , some variations most likely because statistical and systematic errors are visible in detail (Figs. S5 and S6, SM [30]).

The advantage of QENS over other techniques is its ability to probe relaxation times at specific length scales ( $Q$  values), which facilitates the selection of  $Q$  range in which the local diffusion model is valid, i.e.,  $Q > 1 \text{ \AA}^{-1}$ . However, the frequency range of QENS is limited. In order to validate our results, we performed dielectric spectroscopy, which provides a wider range of frequencies, on all samples at different temperatures. The data were shifted using time-temperature superposition (TTS) to obtain master curves at 300 K (Fig. S13, SM [30]). We follow the same procedure as used in QENS to obtain the relaxation time spectra by fitting  $\alpha$  peak. Figure 3(b) shows that further shifted (see below) dielectric relaxation time distributions follow the same trend as QENS relaxation time spectra. NC-5k and NC-12k exhibit both faster and slower relaxations as compared to neat polymers. Owing to the broad range of dielectric spectroscopy, we are able to probe the relaxation times of extremely slow segments too, which only appear as elastic scattering in QENS.

The qualitative agreement between the relaxation time spectra obtained from the two different techniques further supports our results. By a comparison with the backscattering data at  $Q = 1.4 \text{ \AA}^{-1}$  we realize that the spectra need to be shifted more strongly than TTS would prescribe, in order to agree with the QENS timescale. The appropriate factors amount to 0.1 to 0.15. Such additional factors result from

the  $Q$  dependence of the relaxation times in QENS and are well known [40]. Using these phenomenologically shifted dielectric distribution functions leads to an excellent description of the neutron data [Fig. 3(c)], further underlining the quantitative agreement between dielectric and of backscattering results within the proper resolution window. Therefore, with relaxation time spectra analysis of backscattering data, one can accurately probe the actual distribution to about 6 decades of timescales [compare Figs. 3(a) and 3(b)], whereas beyond that dielectric spectroscopy proves to be more accurate.

Furthermore, we note that other than dielectric spectroscopy QENS reflects directly the protonic motions, be it rotational or translational. While dielectric spectroscopy is largely sensitive to bond rotations, neutron spectra with  $\tau^{-1} = D_{\text{local}} Q^2$  directly and quantitatively monitor the local diffusion  $D_{\text{local}}$ ; e.g.,  $\langle D_{\text{local}} \rangle$  for NC-5k at 300 K amounts to  $D_{\text{local}} = 0.43 \times 10^{-11} \text{ m}^2/\text{s}$  (significantly slower than in the neat melt:  $D_{\text{local}} = 0.69 \times 10^{-11} \text{ m}^2/\text{s}$ ).

Above results capture critical features of segmental dynamics along the polymer chain in OCNC. Although the KWW times and  $\tau_o$  show contrasting trends in NC-5k and NC-12k, the implication of grafting on the short time relaxation is remarkably similar in both. Broadly, we notice an increase in the fraction of faster segments (Figs. S7–S12, SM [30]), whereas the distribution of slow-moving segments (at longer times) is substantially different for NC-5k and NC-12k.

Our data, in agreement with other literature reports [7,20,41–43], establish the presence of a decelerated polymer layer next to the nanoparticle surface. In the radial direction from the surface, a gradual change in segmental dynamics from extremely slow to slow and eventually to faster relaxation has to take place. Repercussion of this systematic transition could be observed as retarded dynamics at longer timescales in the relaxation time spectrum. Nevertheless, the length scale over which this transition takes place should be independent of the chain length at a fixed grafting density. Therefore, the number of slower segments in both NC-5k and NC-12k should be comparable. This explains the difference in fractional contribution of slower segments in these two nanocomposites as shown in Fig. 3(a). Due to shorter chains, NC-5k exhibits significantly higher fraction of slow segments than NC-12k which is manifested as broadening of relaxation time distributions at longer times. An increase in  $T_g$  for NC-5k

further supports this finding. In the literature, an increase of  $T_g$  has been observed for ungrafted nanocomposites of C60 and polyisoprene [44], which was interpreted as a consequence of increased segmental friction.

On the other hand, the longer chain length of NC-12k diminishes the contribution of slow segments in the spectra. The higher fraction of faster segments and a decrease in  $T_g$  for NC-12k compared to the neat melt advocate an overall decrease in the segmental packing density similar to the findings on polypropylene glycol/silica nanocomposites [45]. This reasoning allows us to explain the apparently contrasting effects of grafting on the two different molecular weight OCNC. The

implementation of relaxation time distribution analysis clarifies that the effect of grafting on the dynamics of segments occurs in the same manner in both nanocomposites. Thus, our work leads to a rationalization of contradicting results from different studies on OCNCs [7,20,21] and will be helpful in developing more advanced models for these systems.

We acknowledge Amruta Sharma for differential scanning calorimetry measurements and Ralf Biehl for useful discussions.

All authors have given approval to the final version of the manuscript.

- 
- [1] M. R. Bockstaller, Progress in polymer hybrid materials, *Prog. Polym. Sci.* **40**, 1 (2015).
  - [2] B. Sarkar and P. Alexandridis, Progress in polymer science block copolymer–nanoparticle composites: Structure, functional properties, and processing, *Prog. Polym. Sci.* **40**, 33 (2015).
  - [3] C. R. Bilchak, E. Buening, M. Asai, K. Zhang, C. J. Durning, S. K. Kumar, Y. Huang, B. C. Benicewicz, D. W. Gidley, S. Cheng, A. P. Sokolov, M. Minelli, and F. Doghieri, Polymer-grafted nanoparticle membranes with controllable free volume, *Macromolecules* **50**, 7111 (2017).
  - [4] S. K. Kumar, N. Jouault, B. Benicewicz, and T. Neely, Nanocomposites with polymer grafted nanoparticles, *Macromolecules* **46**, 3199 (2013).
  - [5] C. Deng, J. Wu, R. Cheng, F. Meng, and H. Klok, Progress in polymer science functional polypeptide and hybrid materials: Precision synthesis via  $\alpha$ -amino acid N-carboxyanhydride polymerization and emerging biomedical applications, *Prog. Polym. Sci.* **39**, 330 (2014).
  - [6] *Rheology and Processing of Polymer Nanocomposites*, edited by S. Thomas, R. Muller, and J. Abraham (John Wiley & Sons, Inc., Hoboken, NJ, 2016).
  - [7] M. Jhalaria, E. Buening, Y. Huang, M. Tyagi, R. Zorn, M. Zamponi, V. García-Sakai, J. Jestin, B. C. Benicewicz, and S. K. Kumar, Accelerated Local Dynamics in Matrix-Free Polymer Grafted Nanoparticles, *Phys. Rev. Lett.* **123**, 158003 (2019).
  - [8] D. Richter and M. Kruteva, Polymer dynamics under confinement, *Soft Matter* **15**, 7316 (2019).
  - [9] E. J. Bailey and K. I. Winey, Dynamics of polymer segments, polymer chains, and nanoparticles in polymer nanocomposite melts: A review, *Prog. Polym. Sci.* **105**, 101242 (2020).
  - [10] S. Choudhury, S. Stalin, Y. Deng, and L. A. Archer, Soft colloidal glasses as solid-state electrolytes, *Chem. Mater.* **30**, 5996 (2018).
  - [11] G. Kortaberria, P. Arruti, A. Jimeno, I. Mondragon, and M. Sangermano, Local dynamics in epoxy coatings containing iron oxide nanoparticles by dielectric relaxation spectroscopy, *J. Appl. Polym. Sci.* **109**, 3224 (2008).
  - [12] M. Krutyeva, J. Martin, A. Arbe, J. Colmenero, C. Mijangos, G. J. Schneider, T. Unruh, Y. Su, and D. Richter, Neutron scattering study of the dynamics of a polymer melt under nanoscopic confinement, *J. Chem. Phys.* **131**, 174901 (2009).
  - [13] A. Arbe, J. Colmenero, F. Alvarez, M. Monkenbusch, D. Richter, B. Farago, and B. Frick, Experimental evidence by neutron scattering of a crossover from Gaussian to non-Gaussian behavior in the  $\alpha$  relaxation of polyisoprene, *Phys. Rev. E* **67**, 051802 (2003).
  - [14] A. Arbe, J. Colmenero, F. Alvarez, M. Monkenbusch, D. Richter, B. Farago, and B. Frick, Non-Gaussian Nature of the  $\alpha$  Relaxation of Glass-Forming Polyisoprene, *Phys. Rev. Lett.* **89**, 245701 (2002).
  - [15] A. Arbe, J. Colmenero, M. Monkenbusch, and D. Richter, Dynamics of Glass-Forming Polymers: “Homogeneous” versus “Heterogeneous” Scenario, *Phys. Rev. Lett.* **81**, 590 (1998).
  - [16] A. C. Genix, A. Arbe, F. Alvarez, J. Colmenero, B. Farago, A. Wischniewski, and D. Richter, Self- and collective dynamics of syndiotactic poly(methyl methacrylate). A combined study by quasielastic neutron scattering and atomistic molecular dynamics simulations, *Macromolecules* **39**, 6260 (2006).
  - [17] J. Midya, M. Rubinstein, S. K. Kumar, and A. Nikoubashman, Structure of polymer-grafted nanoparticle melts, *ACS Nano* **14**, 15505 (2020).
  - [18] E. J. Bailey, P. J. Griffin, M. Tyagi, and K. I. Winey, Segmental diffusion in attractive polymer nanocomposites: A quasi-elastic neutron scattering study, *Macromolecules* **52**, 669 (2019).
  - [19] D. Dukes, Y. Li, S. Lewis, B. Benicewicz, L. Schadler, and S. K. Kumar, Conformational transitions of spherical polymer brushes: Synthesis, characterization, and theory, *Macromolecules* **43**, 1564 (2010).
  - [20] C. Mark, O. Holderer, J. Allgaier, E. Hübner, W. Pyckhout-Hintzen, M. Zamponi, A. Radulescu, A. Feoktystov, M. Monkenbusch, N. Jalarvo, and D. Richter, Polymer Chain Conformation and Dynamical Confinement in a Model One-Component Nanocomposite, *Phys. Rev. Lett.* **119**, 047801 (2017).
  - [21] S. A. Kim, R. Mangal, and L. A. Archer, Relaxation dynamics of nanoparticle-tethered polymer chains, *Macromolecules* **48**, 6280 (2015).
  - [22] E. U. Mapesa, N. M. Cantillo, S. T. Hamilton, M. A. Harris, Jr, T. A. Zawodzinski, A. H. Alissa Park, and J. Sangoro, Localized and collective dynamics in liquid-like polyethylenimine-based nanoparticle organic hybrid materials, *Macromolecules* **54**, 2296 (2021).
  - [23] X. Liu, B. A. Abel, Q. Zhao, S. Li, S. Choudhury, J. Zheng, and L. A. Archer, Microscopic origins of caging and equilibration of self-suspended hairy nanoparticles, *Macromolecules* **52**, 8187 (2019).

- [24] F. Mohamed, Dynamics of advanced polymer systems studied by dielectric spectroscopy and rheology: From binary glass formers to nanocomposites, Universitaet Bayreuth, Germany, Ph. D. thesis, 2018.
- [25] P. Agarwal, S. A. Kim, and L. A. Archer, Crowded, Confined, and Frustrated: Dynamics of Molecules Tethered to Nanoparticles, *Phys. Rev. Lett.* **109**, 258301 (2012).
- [26] A. P. Holt, V. Bocharova, S. Cheng, A. M. Kisliuk, G. Ehlers, E. Mamontov, V. N. Novikov, and A. P. Sokolov, Interplay between local dynamics and mechanical reinforcement in glassy polymer nanocomposites, *Phys. Rev. Materials* **1**, 062601(R) (2017).
- [27] A. P. Holt and C. M. Roland, Segmental and secondary dynamics of nanoparticle-grafted oligomers, *Soft Matter* **14**, 8604 (2018).
- [28] D. Salatto, J.-M. Y. Carrillo, M. K. Endoh, T. Taniguchi, B. M. Yavitt, T. Masui, H. Kishimoto, M. Tyagi, A. E. Ribbe, V. Garcia Sakai, M. Kruteva, B. G. Sumpter, B. Farago, D. Richter, M. Nagao, and T. Koga, *Structural and Dynamical Roles of Bound Polymer Chains in Rubber Reinforcement*, *ACS Nano* **54**, 11032 (2021).
- [29] S. Ehlert, S. M. Taheri, D. Pirner, M. Drechsler, H. W. Schmidt, and S. Förster, Polymer ligand exchange to control stabilization and compatibilization of nanocrystals, *ACS Nano* **8**, 6114 (2014).
- [30] See Supplemental Material at <http://link.aps.org/supplemental/10.1103/PhysRevMaterials.6.L012601> for grafting density procedure, methyl rotation model, neat polyisoprene dynamics, average relaxation times, differential scanning calorimetry, relaxation time spectra, and dielectric spectroscopy data.
- [31] J. Wuttke, A. Budwig, M. Drochner, H. Kämmerling, F. J. Kayser, H. Kleines, V. Ossovy, L. C. Pardo, M. Prager, D. Richter, G. J. Schneider, H. Schneider, and S. Staringer, SPHERES, Jülich's High-Flux Neutron Backscattering Spectrometer at FRM II, *Rev. Sci. Instrum.* **83**, 075109 (2012).
- [32] R. Biehl, JSCATTER, a program for evaluation and analysis of experimental data, *PLoS One* **14**, e0218789 (2019).
- [33] T. Glomann, G. J. Schneider, J. Allgaier, A. Radulescu, W. Lohstroh, B. Farago, and D. Richter, Microscopic Dynamics of Polyethylene Glycol Chains Interacting with Silica Nanoparticles, *Phys. Rev. Lett.* **110**, 178001 (2013).
- [34] R. Zorn, B. Frick, and L. J. Fetters, Quasielastic neutron scattering study of the methyl group dynamics in polyisoprene, *J. Chem. Phys.* **116**, 845 (2002).
- [35] C. Mark, Structure and dynamics of polymer chains grafted on nanoparticles, Westfälischen Wilhelms-Universität Münster, Ph. D. thesis, 2013.
- [36] J. Colmenero, A. Alegría, A. Arbe, and B. Frick, Correlation between Non-Debye Behavior and Q Behavior of the Relaxation in Glass-Forming Polymeric Systems, *Phys. Rev. Lett.* **69**, 478 (1992).
- [37] F. Alvarez, A. Alegría, and J. Colmenero, Relationship between the time-domain Kohlrausch-Williams-Watts and frequency-domain Havriliak-Negami relaxation functions, *Phys. Rev. B* **44**, 7306 (1991).
- [38] S. W. Provencher, Contin: A general purpose constrained regularization program for inverting noisy linear algebraic and integral equations, *Comput. Phys. Commun.* **27**, 229 (1982).
- [39] I.-G. Marino, Regularized inverse laplace transform, MATLAB, Central File Exchange, Retrieved January 24, 2022, <https://www.mathworks.com/matlabcentral/fileexchange/6523-rilt>.
- [40] *Broadband Dielectric Spectroscopy*, edited by K. Friedrich and A. Schönhal, (Springer Science & Business Media, Springer-Verlag, Berlin, 2003).
- [41] Y. Lin, L. Liu, G. Xu, D. Zhang, A. Guan, and G. Wu, Interfacial interactions and segmental dynamics of poly(vinyl acetate)/silica nanocomposites, *J. Phys. Chem. C* **119**, 12956 (2015).
- [42] B. Carroll, S. Cheng, and A. P. Sokolov, Analyzing the interfacial layer properties in polymer nanocomposites by broadband dielectric spectroscopy, *Macromolecules* **50**, 6149 (2017).
- [43] A. P. Holt, V. Bocharova, S. Cheng, A. M. Kisliuk, B. T. White, T. Saito, D. Uhrig, J. P. Mahalik, R. Kumar, A. E. Imel, T. Etampawala, H. Martin, N. Sikes, B. G. Sumpter, M. D. Dadmun, and A. P. Sokolov, Controlling interfacial dynamics: Covalent, *ACS Nano* **10**, 6843 (2016).
- [44] Y. Ding, S. Pawlus, A. P. Sokolov, J. F. Douglas, A. Karim, and C. L. Soles, Dielectric spectroscopy investigation of relaxation in C 60 - Polyisoprene nanocomposites, *Macromolecules* **42**, 3201 (2009).
- [45] R. Casalini and C. M. Roland, Local and global dynamics in polypropylene glycol/silica composites, *Macromolecules* **49**, 3919 (2016).